Estimating Xenobiotic Half-Lives in Humans from Rat Data: Influence of log P

Jeffrey G. Sarver,[1] Donald White,[1,2] Paul Erhardt,[3] and Kenneth Bachmann[1]

[1]Department of Pharmacology, [2]Department of Mathematics, and [3]Center for Drug Design and Development, The University of Toledo, Toledo, OH 43606 USA

The nature of empirical allometric expressions relating dispositional and kinetic parameters for a given xenobiotic across multiple mammalian species is well known. It has also been demonstrated that a simple allometric relationship may be used to predict kinetic parameters for humans based merely on data for multiple xenobiotics from rats. We decided to explore reasons for the variance in the data arising from the latter method. We were particularly interested in learning whether any physicochemical characteristics of xenobiotics might account for outlying data points (i.e., poor prediction of human half-life from rat half-life). We have explored the influence of lipid solubility as reflected by a xenobiotic's log P value because adipose tissue comprises a significantly larger percentage of total body weight in humans than in rats. We used half-life data from the literature for 127 xenobiotics. A data subset of 102 xenobiotics for which we were able to find estimates of log P values, including several with extremely large log P values, was also analyzed. First and second order models, including and excluding log P, were compared. The simplest of these models can be recast as the familiar allometric relationship having the form $Y = a(X^b)$. The remaining models can be seen as extensions of this relationship. Our results suggest that incorporation of log P into the prediction of xenobiotic half-life in humans from rat half-life data is important only for xenobiotics with extremely large log P values such as dioxins and polychlorinated biphenyls. Moreover, a second order model in logarithm of rat half-life accommodates all data points very well, without specifically accounting for log P values. *Key words*: half-life, log P, scaling, xenobiotics.

Environ Health Perspect 105:1204–1209 (1997). *http//ehis.niehs.nih.gov*

It has recently been demonstrated that half-lives of xenobiotics estimated in rats can be used to predict their half-lives in humans using a linear model that is logarithmic in both variables as follows:

$$\log(t_{1/2h}) = \alpha + [b \log(t_{1/2r})] + e \quad (1)$$

where $t_{1/2h}$ and $t_{1/2r}$ represent xenobiotic half-lives for humans and rats, respectively, for an array of different xenobiotics, and e is an error term assumed to be normally distributed with a constant standard deviation, σ (*1*). This model was derived from a regression analysis of over 100 xenobiotics for which both rat and human half-life values had been reported, and could be simplified to an allometric expression:

$$t_{1/2h} = a\,(t_{1/2r})^b \quad (2)$$

where a depends on both α and e.

The values for rat half-life used in the former analysis ranged from about 0.02 hr to 1,776 hr. It was additionally reported that the 80% confidence intervals for the predicted human half-lives generally embraced about a 10-fold range of predicted half-life values and that the model accounted for 75% of the variance in the relationship between $t_{1/2h}$ and $t_{1/2r}$ (*1*).

In this study, we explored the possibility that accounting for the role of xenobiotic lipid solubility might provide an improvement in the prediction of human half-life values estimated directly from rat half-life data. The lipid solubility of xenobiotics would be expected to be an important parameter in determining the half-life relationship between rats and humans because the adipose content of humans as a percentage of total body weight is 3–4 times larger than for rats (23% vs. 7%, respectively) (*2*). To explore the effect of lipid solubility, we examined the ability of the octanol:water partition coefficient, expressed as log P, to account for some of the variability remaining in the data after use of the simple linear expression in Equation 1. We also expanded the number of substances with high log P values (>6.5) to better evaluate how well this model and others accommodate xenobiotics with such high log P values and hence extremely long half-lives.

Methods

Average half-life values in rats and humans for 127 xenobiotics were obtained from the literature. The references for 103 of those variates have been published [see Bachmann et al. (*1*)]. Log P values for 102 of these xenobiotics were ascertained from one of four resources (*3–6*) and represented a mix of experimentally determined or calculated values. The influence of the log P of a xenobiotic on the accuracy of its predicted human half-life from rat half-life data was investigated as follows.

We successively explored six different models, ranging from the simple to the complex. The models are listed in Table 1. Model 1 can be recognized as a first order Taylor series in one variable, log $t_{1/2r}$. Model 2 is a second order Taylor series in log $t_{1/2r}$. Model 3 is a first order Taylor series in two variables, log $t_{1/2r}$ and log P. Models 4–6 are second order Taylor series' in two variables, log $t_{1/2r}$ and log P.

Two of the models (Models 1 and 2) were evaluated using both the full data set (n = 127) and the more limited data set (n = 102), which included only those substances for which log P values were available.

Models were evaluated using simple regression analysis. The statistical parameters of interest were the root mean square error (RMSE) of the observed versus predicted values; the adjusted R^2 value, which is a measure of the total variance explained by the model; the estimate of each coefficient; and the results of a two-tailed t-test ascertaining whether the coefficient value is significantly different from zero. Differences were considered significant at p-values <0.05. Computations, including regression analyses, were performed using SAS statistical software (SAS Institute, Cary, NC) running on an IBM 9672 mainframe computer (IBM, Somers, NY).

Results

Results of the regression analyses and t-test are given in Table 1. For the models that do not take specific account of log P (Models 1 and 2), it should be noted that the quadratic model is preferred (Model 2). This becomes apparent when comparing the graphs of Models 1 and 2 for the full data set (Fig. 1), where it can be seen that Model 2 better accomodates xenobiotics with extremely high values of $t_{1/2r}$, which also tend to be xenobiotics with extremely large (≥6.5) values for log P. Model 3 is a first-order Taylor series in both log $t_{1/2r}$ and log P, and it yields less satisfactory results than Model 2 when applied to the same data set (i.e., the 102 xenobiotics for which log P values were available). For comparative purposes, Model

Address correspondence to K. Bachmann, Department of Pharmacology, The University of Toledo College of Pharmacy, 2801 W. Bancroft St., Toledo, OH 43606 USA.

The authors thank Osama Salouha for his assistance.
Received 18 February 1997; accepted 14 July 1997.

Table 1. Statistical results of six models used to predict human half-life from rat half-life data

Model	Equation	Number	RMSE	R^2 (adjusted)	Coefficient	Coefficient estimate and (SE)	*p*-Value
1	$\log t_{1/2h} = a + b(\log t_{1/2r})$	127	0.4276	0.8312	a	0.7174 (0.0390)	0.0001
					b	1.0718 (0.0430)	0.0001
		102	0.4589	0.8251	a	0.7480 (0.0469)	0.0001
					b	1.0825 (0.0495)	0.0001
2	$\log t_{1/2h} = a + b_1(\log t_{1/2r}) + b_2(\log t_{1/2r})^2$	127	0.3803	0.8662	a	0.6342 (0.0376)	0.0001
					b_1	0.8697 (0.0517)	0.0001
					b_2	0.1523 (0.0262)	0.0001
		102	0.4038	0.8646	a	0.6573 (0.0444)	0.0001
					b_1	0.8273 (0.0637)	0.0001
					b_2	0.1679 (0.0306)	0.0001
3	$\log t_{1/2h} = a + b(\log t_{1/2r}) + c(\log P)$	102	0.4288	0.8474	a	0.6180 (0.0548)	0.0001
					b	0.9504 (0.0571)	0.0001
					c	0.0850 (0.0216)	0.0001
4	$\log t_{1/2h} = a + b_1(\log t_{1/2r}) + b_2(\log t_{1/2r})^2 + c_1(\log P)$	102	0.3885	0.8747	a	0.5775 (0.0504)	0.0001
					b_1	0.7668 (0.0643)	0.0001
					b_2	0.1445 (0.0304)	0.0001
					c_1	0.0604 (0.0202)	0.0035
5	$\log t_{1/2h} = a + b_1(\log t_{1/2r}) + b_2(\log t_{1/2r})^2 + c_1(\log P) + c_2(\log P)^2$	102	0.3871	0.8756	a	0.5747 (0.0503)	0.0001
					b_1	0.7842 (0.0651)	0.0001
					b_2	0.1600 (0.0325)	0.0001
					c_1	0.0912 (0.0309)	0.0039
					c_2	-0.0007(0.0058)	0.1914
6	$\log t_{1/2h} = a + b_1(\log t_{1/2r}) + b_2(\log t_{1/2r})^2 + c_1(\log P) + c_2(\log P)^2 + d(\log t_{1/2r})(\log P)$	102	0.3837	0.8777	a	0.6010 (0.0523)	0.0001
					b_1	0.7009 (0.0821)	0.0001
					b_2	0.1158 (0.0419)	0.0069
					c_1	0.1138 (0.0335)	0.0010
					c_2	-0.0178(0.0084)	0.0377[a]
					d	0.0490 (0.0298)	0.1033[a]

Abbreviations: RMSE, root mean square error; SE, standard error.
[a]The *p*-value for these two coefficients together (i.e., collectively) is 0.1128.

2 is graphed in juxtaposition to Model 1 in Figure 1. Model 2 is graphed with prediction intervals in Figure 2; in this figure the full data set was used.

Models 4, 5 and 6 use $t_{1/2r}$ and log P in various second order Taylor series models to predict human half-life. These three models are virtually equivalent in terms of RMSE and adjusted R^2, differing by little more than 1% from one another in RMSE and less for R^2. This fact alone leads us to select the least complex model among these, Model 4. In addition, we note in Model 6 (the full quadratic model) that the interaction term is not statistically significant, and when that term is dropped (resulting in Model 5), the $(\log P)^2$ term becomes nonsignificant as well. Finally, when the statistical significance of these two terms is jointly tested in Model 6, the *p*-value for the *F*-test is found to be 0.113, as noted in Table 1. Each of these observations lead us to prefer Model 4 out of all models incorporating log P. In Figure 3 the predicted human half-lives are plotted against actual human half-lives. Predictions are based on Models 1–4, and the juxtapositioning of the regression and identity lines is shown. On the basis of the values of the coefficients and exponents for the regression equations, the regression lines for Models 2 and 4 more closely approximate

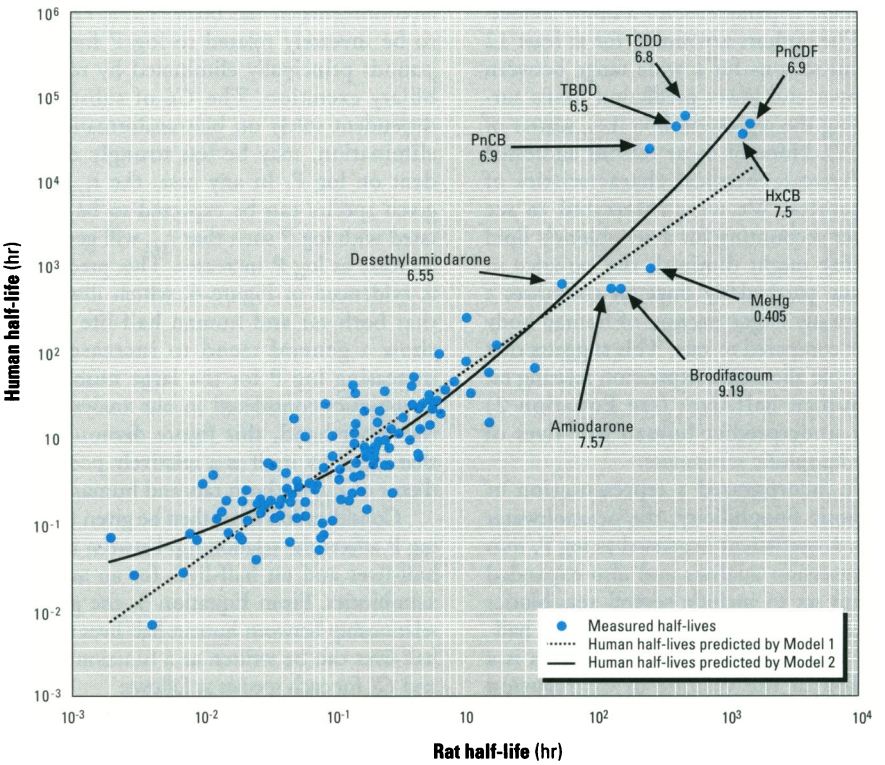

Figure 1. Comparison of the measured human half-lives to human half-lives predicted from rat half-lives by Model 1 and Model 2 for the full data set (n = 127). See Table 1 for model equations and model parameter values. The identity and log P value are indicated for the nine compounds with the highest log P values and/or longest half-lives. Abbreviations: MeHg, methylmercury; PnCB, 2,2′,4,5,5′-pentachlorobiphenyl; TBDD, 2,3,7,8-tetrabromodibenzo-*p*-dioxin; TCDD, 2,3,7,8-tetrachlorodibenzo-*p*-dioxin; PnCDF, 2,3,4,7,8-pentachlorodibenzo-*p*-dioxin; HxCB, 2,2′,4,4′,5,5′-hexachlorobiphenyl.

the identity lines. Similar plots for Models 5 and 6 appear virtually identical to that of Model 4 (not shown).

We also observe that the RMSE and R^2 values for Model 4 appear close to those found for Model 2. This indicates that valid predictions can be obtained even if log P is not available and the prediction is based entirely on $t_{1/2r}$. On the other hand, when only the limited data set (of xenobiotics with log P values available) is used, we find that as log P is considered, RMSE is lower, R^2 is higher, and log P is statistically significant ($p = 0.020$). Thus when log P is available, these results indicate that it is sensible to employ it.

Discussion

Previously, it was reported that reasonably good predictions of human half-lives were possible based exclusively on rat half-life data (*1*). The predictive equation along with upper and lower confidence limits (80%, 90%, and 95%) were derived from a regression analysis based upon human and rat half-life values for 103 xenobiotics and therefore differed from other allometrically based predictions of toxicokinetic parameters in humans for a given xenobiotic, which depend upon the extrapolation across multiple species of the estimates of a toxicokinetic parameter for a single xenobiotic. The authors accounted for at least 12 different reasons for a wide range between the upper and lower prediction limits surrounding the regression line (i.e., scatter of data) (*1*). None of those reasons addressed the physical–chemical characteristics of xenobiotics. We were interested to see whether accounting for a xenobiotic's lipid solubility might diminish the variance in the data, particularly since fat comprises a significantly larger fraction of human body weight compared to rats. This suggests that the simple allometric expression relating rat and human half-lives (see Equation 2) might underpredict human half-lives of highly lipophilic substances.

We incorporated a representation of xenobiotic lipophilicity, the octanol:water partition coefficient expressed as log P, into our regression analysis and also expanded the data set to include several xenobiotics with extremely large log P values. The half-life of a xenobiotic in rats or humans is a function of the volume of distribution (V_D) and the total clearance rate (CL) as given by the equation:

$$t_{1/2} = 0.693\ V_D / CL \qquad (3)$$

V_D is expected to increase with increasing log P as more of the compound is distributed into adipose tissues and other lipid

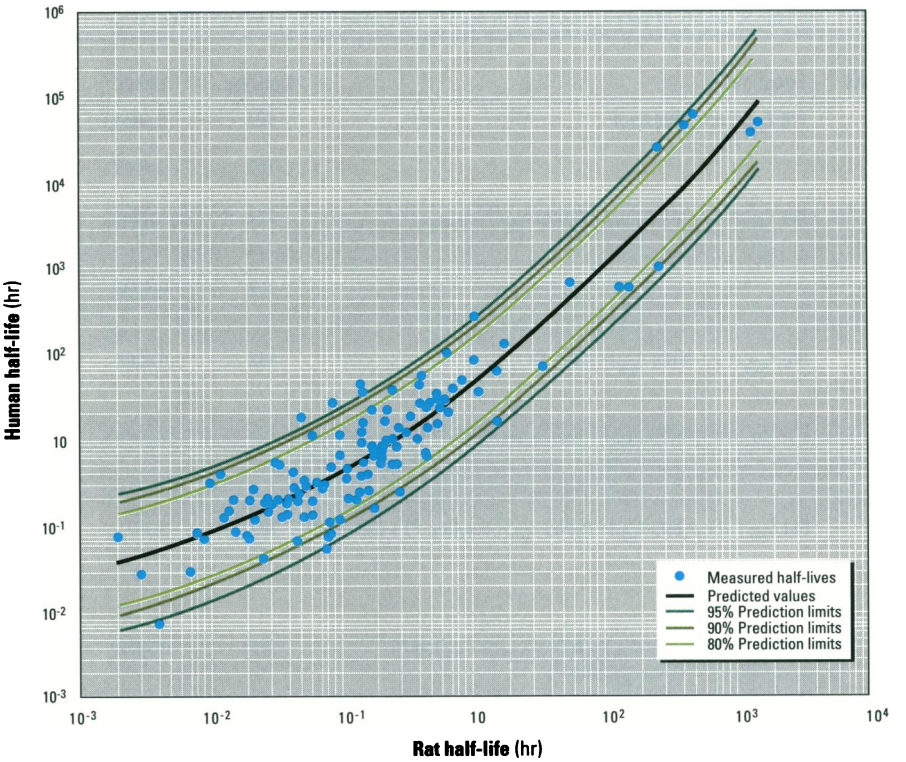

Figure 2. Actual human half-lives and human half-life prediction intervals plotted as a function of rat half-lives for the fit of Model 2 to the full data set ($n = 127$). Curves represent the predicted values, the 95% prediction limits, the 90% prediction limits, and the 80% prediction limits.

environments of the body. CL is expected to be inversely related to log P for compounds principally eliminated by renal or biliary excretion. The CL of substances, dependent solely on biotransformation for elimination, may be less strongly dependent on log P. In any case, the $t_{1/2}$ for a given species can be expected to be correlated with log P such that $t_{1/2}$ will generally increase as log P increases. This prediction is evidenced in Figure 4, which illustrates that both rat and human half-life values show a general trend to increase with increasing log P for the large number of xenobiotics considered in our analysis. On the other hand, this figure demonstrates that log P by itself is a relatively poor predictor of $t_{1/2}$ for both rats and humans.

Consideration must then be given to how log P affects the relationship between human half-lives and rat half-lives for an array of xenobiotics. From Equation 3, the general relationship between human half-lives and rat half-lives can be written as a function of V_D and CL for each species as follows:

$$t_{1/2h} = t_{1/2r}\,(V_{Dh}/V_{Dr})(CL_r/CL_h) \qquad (4)$$

For a given xenobiotic, the CL ratio can be expected to be at least partly correlated with relative body size (*7,8*), but not systematically affected by log P. Because of a higher adipose fraction in humans (23% for humans vs. 7% for rats), however, the human V_D can be expected to increase more with increasing log P than does the rat V_D. The V_D ratio, and hence the ratio of human to rat half-life, should then be generally larger for xenobiotics with high log P values than low log P values. This is indicated in Figure 4, where the disparity between rat and human half-lives is seen to increase for substances with large log P values. Explicitly accounting for log P can, in fact, improve the accuracy of human half-life predictions from rat half-life data as noted by the improved predictions of both Models 3 and 4 versus Models 1 and 2, respectively, when the same data set (i.e., $n = 102$) is used. Because rat half-life is at least partially a function of log P (see Fig. 4), there may be sufficient information within an array of rat half-lives to predict human half-lives across the full range of log P values. This explains why the use of the quadratic equation (Model 2) yielded RMSE values and coefficients of determination roughly comparable to those of Model 4, suggesting that the quadratic equation can be effectively applied to the prediction of xenobiotic half-lives in humans from rat half-life data, even for xenobiotics that possess extremely long half-lives and/or extremely large log P values such as dioxins and polychlorinated biphenyls. Moreover, Model 2 does not even require knowledge of log P values; it only requires a measure of xenobiotic half-life in the rat. It

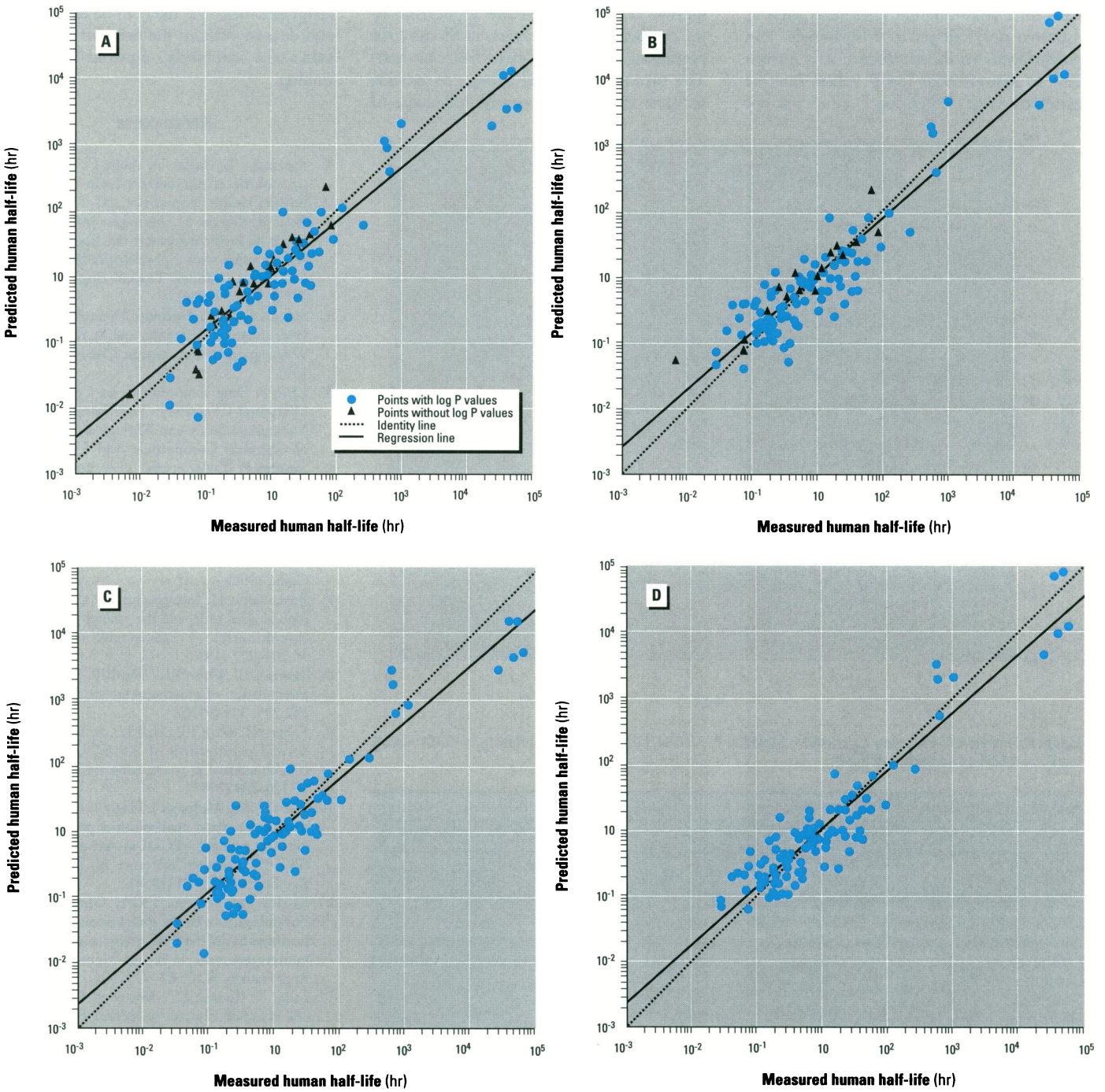

Figure 3. Predicted human half-lives versus measured human half-lives. Predictions based on four models are shown as follows: (A) Model 1 [$y = 1.4074\ (x^{0.8187})$]; (B) Model 2 [$y = 1.2449\ (x^{0.87787})$]; (C) Model 3 [$y = 1.4118\ (x^{0.85039})$]; and (D) Model 4 [$y = 1.3236\ (x^{0.8784})$]. Equations for each regression were computed in all cases only on the subset of data for which log P values were known ($n = 102$); however, additional data points (for which log P values were not known) are also exhibited in Model 1 and Model 2. The dashed line is the zero residual or identity line, which represents a perfect fit.

must be noted that Model 1 appears to break down for xenobiotics with extremely large log P (or half-life) values, and for such substances, the magnitude of human half-lives can be greatly underpredicted by Model 1. It might also be noted that methyl mercury, with a low log P but a long half-life due to unusual binding properties, is well accomodated by this same model.

As a practical matter, we found that accounting for lipid solubility does improve the accuracy of predictions of human xenobiotic half-lives from rat half-life data and decreases variance when log P values are included in the prediction equation. (compared to Model 4 versus Model 2 for equal sample size). This is especially important when predicting human half-lives from rat half-lives for xenobiotics with extremely large log P values (>6.5), where Model 1 (from which the simple allometric expression in Equation 2 is derived) can become inaccurate (see Fig. 1 and Fig. 3A). Thus, Model 4 should be used whenever log P and rat half-life data are both readily available. In many cases, however, log P values may not be known *a priori* for the molecule of interest.

And for environmental chemicals such as dioxins, polyhalogenated biphenyls, and polyhalogenated dibenzofurans, it is reasonable to assume that log P values may be extremely large. When log P values are not known, we recommend the application of the quadratic equation shown in Model 2 for predicting human half-lives from rat half-lives because this model appears to provide accurate predictions over the full range of xenobiotic half-lives likely to be encountered and does so without the need for an explicit value of a xenobiotic's aqueous/lipid partitioning.

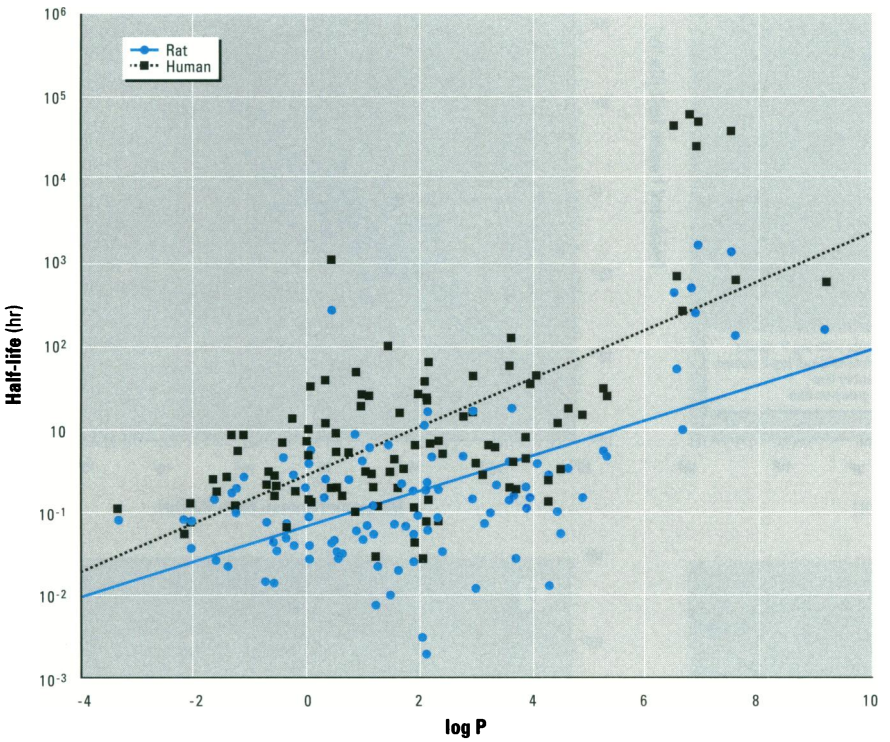

Figure 4. Human half-lives (log $t_{1/2}$ = 0.452 + 0.288 log P; r = 0.647) and rat half-lives (log $t_{1/2}$ = -0.161 + 0.209 log P; r = 0.568) as a function of log P.

Appendix. Tabulation of half-lives in rats and humans

Xenobiotic	$t_{1/2}$ in rat (hr)	Reference	$t_{1/2}$ in human (hr)	Reference
2,2′,4,4′,5,5′ PCB	1,359	(9)	8,112	(10)
2,3,4,7,8 PCDF	1,531	(10)	47,888	(10)
2-Butoxyethanol	0.19	(11)	0.71	(11)
Amiodarone	131	(12)	600	(13)
Barnidipine	0.6	(14)	1.9	(14)
Chlorzoxazone	0.55	(15)	1–13	(16)
Desethylamiodarone	54.8	(17)	674	(18)
Digoxin-specific Fab	3.1	(19)	12.1	(20)
Ethylene glycol	1.7	(21,22)	8.4	(23)
Ethylene oxide	0.2	(24)	0.7	(25)
IND 966	6.6	(26)	21	(26)
Inulin	0.35	(27)	1.23	(28,29)
MTBE	0.5	(30)	19	(31)
Recombinant human factor VIII	5.5	(32)	15.8	(32)
Styrene	0.12	(33)	3.90	(34)
Tamoxifen	10.3	(35)	264	(36)
PCDD (2,3,7,8-TCDD)	484	(10)	62,196	(10)
tert-Butyl alcohol	2.5	(30)	10.2	(31)
Thiopental	2.07	(37)	9	(38)
Tolcapone	0.53	(39)	1.3	(39)
Trovafloxacin	2.2	(40)	9.9	(41)
BSH	4.82	(42)	27	(42)
2,3,7,8 TBDD	430	(10)	43,800	(43)
2,2′,4,5,5′ PCB	256.7	(44)	25,054	(45)

Abbreviations: PCB, polychlorinated biphenyl; PCDF, polychlorinated dibenzofuran; MTBE, methyl *tert*-butyl ether; PCDD, polychlorinated dibenzodioxin; BSH, sodium mercaptoundecahydrododecaborate; TBDD, 2,3,7,8-tetrabromodibenzo-*p*-dioxin.

References

1. Bachmann K, Pardoe D, White D. Scaling basic toxicokinetic parameters from rat to man. Environ Health Perspect 104:400–407 (1996).
2. Reitz R, Gargas M, Andersen M, Provan W, Green T. Predicting cancer risk from vinyl chloride exposure with a physiologically-based pharmacokinetic model. Toxicol Appl Pharmacol 137:253–267 (1996).
3. Hansch C, Leo A, Hoekman D. Exploring QSAR: Hydrophobic, Electronic, and Steric Constants. Washington, DC:American Chemical Society, 1995.
4. Craig P. Drug compendium. In: Comprehensive Medicinal Chemistry: The Rational Design, Mechanistic Study and Therapeutic Application of Chemical Compounds, Vol 6 (Hansch C, Sammes P, Taylor J, eds). New York:Pergamon Press,1990;237–965.
5. Environmental Science Center, Syracuse Research Corporation. http://esc.syrres.com (1996).
6. Leo A, Hansch C, Hoekman D. MacLogP Database, version 2.0. Claremont, CA:Biobyte Corp., 1996.
7. Boxenbaum H. Interspecies scaling, allometry, physiological time, and the ground plan of pharmacokinetics. J Pharmacokin Biopharm 10:201–227 (1982).
8. Travis CC, White RK, Ward RC. Interspecies extrapolation of pharmacokinetics. J Theor Biol 142:285–304 (1990).
9. Fisher HL, Shah PV, Hall LL. *In vivo* and *vitro* dermal penetration of 2,4,5,2′,4′,5′ hexachlorobinphenyl in young adult rats. Environ Res 50:120–139 (1989).
10. Van der Berg M, Jongh J, Poiger H, Olson J. The toxicokinetics and metabolism of polychlorinated dibenzo-*p*-dioxins (PCDDs) and dibenzofurans (PCDFs) and their relevance for toxicity. Crit Rev Toxicol 24:1–74 (1994).
11. Corley RA, Bormett GA, Ghanayem BI. Physiologically based pharmacokinetics of 2-butoxyethanol and its major metabolite, 2-butoxyacetic acid, in rats and humans. Toxicol Appl Pharmacol 129:61–79 (1994).
12. Laine K, Kivisto, KT, Neivonen PJ. Failure of oral activated charcoal to accelerate the elimination of amiodarone and chloroquine. Hum Exp Toxicol 11:491–494 (1992).
13. Gill J, Heel RC, Fitton A. Amiodarone: an overview of its pharmacological properties and review of its therapeutic use in cardiac arrhythmias. Drugs 43:69–110 (1992).
14. Teramura T, Watanabe T, Higuchi S, Hashimoto K. Pharmacokinetics of barnidipine hydrochloride, a new dihydropyridine calcium channel blocker, in the rat, dog, and human. Xenobiotica 25: 1237–1246 (1995).
15. Chen L, Yang C. Effects of cytochrome P4502E1 modulators on the pharmacokinetics of chlorzoxazone and 6-hydroxychlorzoxazone in rats. Life Sci 58:1575–1585 (1996).
16. Bachmann K, Sarver J. Chlorzoxazone as a single sample probe of hepatic CYP2E1 activity in humans. Pharmacology 52:169–177 (1996).
17. Kharidia J, Eddington ND. Effects of desethylamiodarone on the electrocardiogram in

conscious freely moving animals. Pharmaco-kinetic and pharmacodynamic modeling using computer-assisted radio telemetry. Biopharm Drug Dispos 17:93–106 (1996).
18. Ujhelyi M, Klamens K, Vadei K, O'Rangers E, Izard M, Neefe L, Zimmerman J, Chow M. Disposition of intravenous amiodarone in subjects with normal and impaired renal function. J Clin Pharmacol 36:122–130 (1996).
19. Grene-Lerouge N, Bazin-Redureau M, Debray M, Scherrmann J. Interspecies scaling of clearance and volume of distribution for digoxin-specific fab. Toxicol Appl Pharmacol 138:84–89 (1996).
20. Thanh-Barthet CV, Urtizberea M, Sabouraud AE, Cano NJ, Schermann JM. Development of a sensitive radioimmunoassay for fab fragments: application to fab pharmacokinetics in humans. Pharm Res 10:692–696 (1993).
21. Lave T, Dupin S, Schmitt M, Kapps M, Meyers J, Morgenroth B, Chou RC, Jaeck D, Coassolo P. Interspecies scaling of tolcapone, a new inhibitor of catechol-o-methyltransferase (COMT). Use of *in vitro* data from hepatocytes to predict metabolic clearance in animals and humans. Xenobiotica 8:839–851 (1996).
22. Frantz SW, Beskitt JL, Tallant MJ, Zourelias LA, Ballantyne B. Pharmacokinetics of ethylene glycol III. Plasma disposition and metabolic fate after single increasing intravenous, peroral, or percutaneous doses in the male Sprague-Dawley rat. Xenobiotica 26:515–539 (1996).
23. Jacobson D, Hewlett TP, Webb R, Brown ST, Ordinario AT, McMartin KE. Ethylene glycol intoxication: evaluation of kinetics and crystalluria. Am J Med 84:145–152 (1988).
24. Brown C, Wong B, Fennell T. *In vivo* and *in vitro* kinetics of ethylene oxide metabolism in rats and mice. Toxicol Appl Pharmacol 136:8–19 (1996).
25. Filser JG, Denk B, Tornqvist W, Ehrenberg L. Pharmacokinetics of ethylene in man; body burden with ethylene oxide and hydroxyethylation of hemoglobin due to endogenous and environmental ethylene. Arch Toxicol 66:157–163 (1992).
26. Anonymous. Clinical Investigator's Information Brochure for IND 966. New Jersey, 1995.
27. Sarver JG. Development of a tracer technique that utilizes a physiological pharmacokinetic model to quantitatively assess the change in mass transfer rates associated with vascular growth and the application of this technique to the evaluation of a novel bioartifical organoid [Ph.D. dissertation]. The University of Toledo, Toledo, Ohio, 1994.
28. Prescott L, McAuslane J, Freestone S. The concentration-dependent disposition and kinetics of inulin. Eur J Clin Pharmacol 40:619–624 (1991).
29. Freestone S, McAuslane JA, Prescott LF. Effects of tenoxicam on renal function and the disposition of inulin and p-aminohippurate in healthy volunteers and patients with chronic renal failure. Br J Clin Pharmacol 32:495–500 (1991).
30. Borghoff SJ, Murphy JE, Medinsky MA. Development of a physiologically based pharmacokinetic model for methyl tertiary-butyl ether and tertiary-butanol in male Fischer-344 rats. Fundam Appl Toxicol 30:264–275 (1996).
31. Johnson G, Nihlen A, Lof A. Toxicokinetics and acute effects of MTBE and ETBE in male volunteers. Toxicol Lett 82/83:713–718 (1995).
32. Mordenti J, Osaka G, Garcia K, Thomsen K, Licko V, Meng G. Pharmacokinetics and interspecies scaling of recombinant human factor VIII. Toxicol Appl Pharmacol 136:75–78 (1996).
33. Filser JG, Schwegler U, Csanady GA, Greim H, Kreuzer PE, Kessler W. Species-specific pharmacokinetics of styrene in rat and mouse. Arch Toxicol 67:517–530 (1993).
34. Brugnone F, Perbellini L, Wang GZ, Maranelli G, Raineri E, DeRosa E, Saletti C, Soave C, Romeo L. Blood styrene concentrations in a "normal" population and in exposed workers 16 hours after the end of the work shift. Int Arch Occup Environ Health 65:125–130 (1993).
35. Robinson SP, Langan-Fahey SM, Johnson DA, Jordan VC. Metabolites, pharmacodynamics, and pharmacokinetics of tamoxifen in rats and mice compared to the breast cancer patient. Drug Metab Dispos 19:36–43 (1991).
36. Lonning PE, Lien EA, Lundgren S, Kvinnsland S. Clinical pharmacokinetics of endocrine agents used in advanced breast cancer. Clin Pharmacokinet 22:327–358 (1992).
37. Ebling WF, Wada DR, Stanski DR. From piecewise to full physiologic pharmacokinetic modeling:applied to thiopental disposition in the rat. J Pharmacokinet Biopharm 22:259–292 (1994).
38. Homer TD, Stanski DR. The effect of increasing age on thiopental disposition and anesthetic requirement. Anesthesiology 62:714–724 (1985).
39. Lave T, Dupin S, Schmitt M, Kapps M, Meyers J, Morgenroth B, Chou RC, Jaeck D, Coassolo P. Interspecies scaling of tolcapone, a new inhibitor of catechol-o-methyltransferase (COMT). Use of *in vitro* data from hepatocytes to predict metabolic clearance in animals and humans. Xenobiotica 8:839–851 (1996).
40. Teng R, Girard D, Gootz TD, Flouds G, Liston T. Pharmacokinetics of trovafloxacin (CP-99,219), a new quinolone, in rats, dogs and monkeys. Antimicrob Agents Chemother 40:561–566 (1996).
41. Teng R, Harris SC, Nix DE, Schentag JJ, Flouds G, Liston TE. Pharmacokinetics and safety of trovafloxacin (CP-99,219), a new quinolone antibiotic, following administration of single oral doses to healthy male volunteers. J Antimicrob Chemother 36:385–394 (1995).
42. Metha S, Lu D. Interspecies pharmacokinetic scaling of BSH on mice, rats, rabbits, and humans. Biopharm Drug Dispos 16:735–744 (1995).
43. Weber LWD, Greim H. The toxicity of brominated and mixed-halogenated dibenzo-*p*-dioxins and dibenzofurans: an overview. J Toxicol Environ Health 50:195–215 (1997).
44. Matthews HB, Andersen MW. Effect of chlorination on the distribution and excretion of polychlorinated biphenyls. Drug Metab Dispos 3:371–380 (1975).
45. Shirai JH, Kissel JC. Uncertainty in estimated half-lives of PCBs in humans: impact on exposure assessment. Sci Total Environ 187:199–210 (1996).